DOI: 10.1002/ejic.201100160

Guanidino-Functionalised Aromatic Electron Donors at Work: Competing Hydrogen- and Electron-Transfer Reactions in the Course of the Synthesis of Gold Acetylide Complexes

Dimitri Emeljanenko,[a] Elisabeth Kaifer,[a] and Hans-Jörg Himmel*[a]

Keywords: Gold / Guanidine / C-H acidity / Acetylides / Electron transfer / Anions

In this work reactions between [AuCl(PPh$_3$)] and HC≡CAr (Ar = phenyl, pyridinyl, biphenyl or *p*-acetylphenyl) in the presence of the nitrogen base and organic electron donor 1,2,4,5-tetrakis(*N*,*N*′-dimethyl-*N*,*N*′-ethyleneguanidino)benzene (**1**) were studied. Two different product types were isolated and characterised: the neutral Au^{I} acetylides [Au(C≡CAr)PPh$_3$] and the salts (**1**)[Au(C≡CAr)$_2$]$_2$. They can be easily separated from each other by crystallisation under different conditions. The yields strongly depend on the applied acetylene. While the first product type underlines the basic properties of **1**, the second product type highlights its electron-donor capacity. The experimental results indicate reduction of the C−H protons to H$_2$ and two-electron oxidation of **1**. Thermal decomposition of (**1**)[Au(C≡CAr)$_2$]$_2$ (Ar = Ph) leads back to the neutral guanidine and Au nanoparticles (accompanied by oxidative coupling of the two acetylide ligands).

Introduction

Because of their simple structure, [AuX$_2$]$^-$ anions are applied as building blocks in supramolecular structures. In particular, bis(acetylido)Au^{I} complexes, which often feature Au–Au contacts, have been studied intensively, and they generally exhibit interesting optical properties.[1,2] A versatile access route to these species is provided by the "acac method".[3] It starts with [Au(acac)$_2$]$^-$ (acac = acetylacetonato), which is brought to reaction, e.g. with HCCAr (Ar = aryl group), according to Scheme 1. Although a variety of bis(acetylido)Au complexes were synthesised according to this route,[4] it has some limitations. As mentioned by Vicente and Chicote,[4] the presence of acetylacetone in the reaction mixture could lead to the formation of oily products when the solvent is removed. However, this problem only occurs in a very limited number of cases and could be relatively easily solved. A more severe problem arises if the acidic acetylacetone induces successive reactions.

Scheme 1.

Recently, we reported on the reaction between CH$_3$CN and the Au^{I} complex [AuCl(PPh$_3$)] in the presence of the guanidine base **1** [1,2,4,5-tetrakis(*N*,*N*′-dimethyl-*N*,*N*′-ethyleneguanidino)benzene, see Scheme 2], yielding the first structurally characterised cyanomethyl complex of gold, [Au(CH$_2$CN)PPh$_3$].[5] This reaction can hardly be explained simply by an acid-base reaction between the C−H-acidic CH$_3$CN and the N-base **1**, since the basicity of **1** (pK_a = 23.8 in CH$_3$CN) appears to be too low to generate significant amounts of CH$_2$CN$^-$. Acetonitrile solutions of **1** indeed showed no sign of solvent deprotonation. More intriguing, the reaction does not work if **1** is replaced by the *stronger* base **2** [1,2,4,5-tetrakis(tetramethylguanidino)benzene, see Scheme 2, pK_a = 25.3 for **2** in CH$_3$CN].[6]

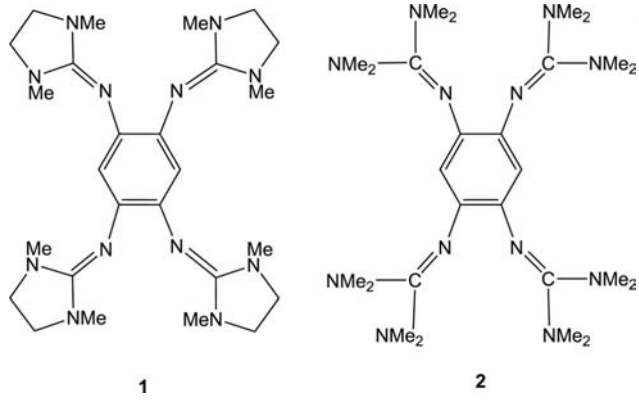

Scheme 2.

Based on the experimental results, we therefore proposed that the reaction can be regarded as a combination between deprotonation by the N-base **1** and C−H activation by Au^{I}.[6] Bright-yellow crystals formed containing the [Au(CH$_2$CN)PPh$_3$] units together with 0.5 equiv. of neutral

[a] Anorganisch-Chemisches Institut, Ruprecht-Karls-Universität Heidelberg,
Im Neuenheimer Feld 270, 69120 Heidelberg, Germany
Fax: +49-6221-545707
E-mail: hans-jorg.himmel@aci.uni-heidelberg.de

Supporting information for this article is available on the WWW under http://dx.doi.org/10.1002/ejic.201100160.

1. The crystals melt at 170 °C and decompose at 207 °C with elimination of the PPh_3 units. Surprisingly, an oxidation of **1**, which represents a strong organic two-electron donor (see Scheme 3) does not occur, even at high temperatures. Motivated by these results and considerations, we are currently studying in more detail the reactions of [AuCl(PPh_3)] with C−H acids mediated by **1** and related guanidino-functionalised aromatic compounds. In this work we report on the reaction between [AuCl(PPh_3)] and acetylenes HC≡CAr (Ar = aryl group) in the presence of **1**. We will see that the electron donor and the Brønsted base properties of **1** compete with each other. The products of the redox reactions are salts containing $\mathbf{1}^{2+}$ and $[AuX_2]^-$ (X = acetylide) units.

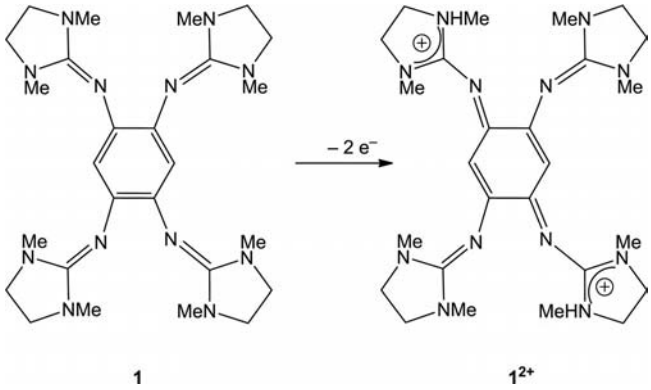

Scheme 3.

Results and Discussion

Scheme 4 shows the Lewis structures of the acetylenes used in this work together with their notation. The discussion is divided into two sections. In the first, the reactions and the structural characterisation of the products are presented. In the second part we report on the thermal stability and optical properties of one of the bis(acetylido)Au products.

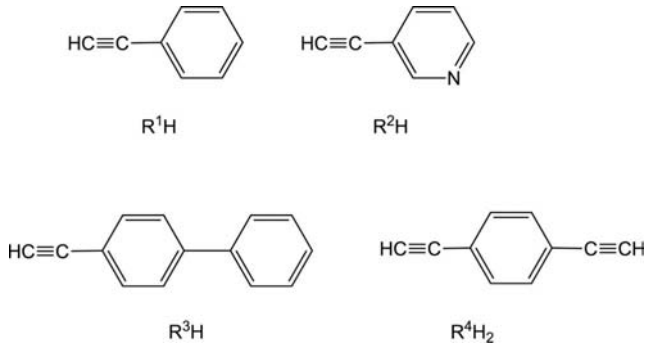

Scheme 4.

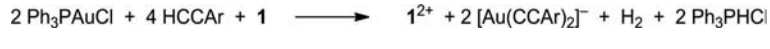

Scheme 5.

Synthesis and Structural Characterisation

In all experiments, the Au^I complex [AuCl(PPh_3)] was treated with an excess of acetylene and 0.5 equiv. of **1** in CH_3CN. Although CH_3CN was shown to be reactive in our previous work,[6] the experiments indicate that CH_3CN deprotonation does not occur in the presence of acetylenes in the solution. Two types of products were isolated. The first type (denoted type I in the following) consists of neutral (acetylido)gold complexes [Au(C≡CAr)PPh_3], arising from deprotonation of the acetylene by **1** (or, as in the case of CH_3CN,[6] a combination of deprotonation by **1** and C−H activation by Au^I). The second isolated product type (denoted type II in the following) consists of salts of the general formula (**1**)[Au(C≡CAr)$_2$]$_2$, featuring oxidised guanidines **1** and bis(acetylido)Au^I anions. Intriguingly, guanidine oxidation is observed in the case of the relatively strong C−H acidic acetylenes but not at all (even at elevated temperatures) in the case of the weaker C−H acid CH_3CN.[6] Oxidation of **1** is accompanied by hydrogen reduction to give H_2. This was shown by passing the gas evolved during the reaction through a CH_3OH solution of $PdCl_2$ leading to a black Pd precipitate.[7] In addition, the ^{31}P NMR spectra showed a signal at δ = 23.17 ppm characteristic of the cation $[Ph_3PH]^+$. Elemental gold was not formed. Thus, the reaction leading to product type II can be expressed by the equation given in Scheme 5.

The relative yields of the product types I and II vary with the applied acetylene. In the case of R^1H, we found 47% of product type I and 41% of type II. The yields decrease to 37% of type I and 33% of type II in the case of R^2H. Finally, for R^3H we obtained 13% of product type I and only 2% of type II. In the case of reaction with R^4H, not more than a few crystals of product type II were isolated. The two product types can easily be separated from each other by crystallisation under different conditions (see Experimental Section). Although the reactions were carried out in CH_3CN as solvent, we did not find any sign of solvent deprotonation (the only exception being the reaction with R^1H, for which mass spectra showed an extremely weak signal due to [Au(CH_2CN)PPh_3]). In the reactions with low yield (especially reaction of R^4H), the reaction mixture contained large amounts of unreacted starting compounds.

[Au(C≡CAr)(PPh_3)] (Type I)

The structures determined for the (acetylido)Au^I complexes [Au(R^1)PPh_3] and [Au(R^2)PPh_3] are illustrated in Figure 1. Of these, the crystal structure of [Au(R^1)PPh_3] has already been reported.[8] However, our analysis of new X-ray diffraction data resulted in significantly different structural parameters. Whereas the space group $P2_1/c$ was reported in the previous study, our analysis found the space

group *C*2/*c*. Most importantly, the Au···Au separation measures 295.06(6) pm according to our analysis. The previous study found a much larger separation of 337.9(1) pm. The Au–P and Au–C distances [228.52(11) and 199.5(3) pm] are similar to those reported previously. Dimeric units are also formed in the Au^{I} complex [Au(R^2)(PPh_3)]. The Au···Au contacts measure 327.74(14) pm. The structure of [Au(R^3)PPh_3] was previously determined,[9] and our structural data (see Supporting Information) are in agreement with the literature data. The shortest Au···Au separation is already 586.8(3) pm long. Thus, [Au(R^3)PPh_3] does not form dimeric assemblies in the solid state, in contrast to [Au(R^1)PPh_3] and [Au(R^2)PPh_3].

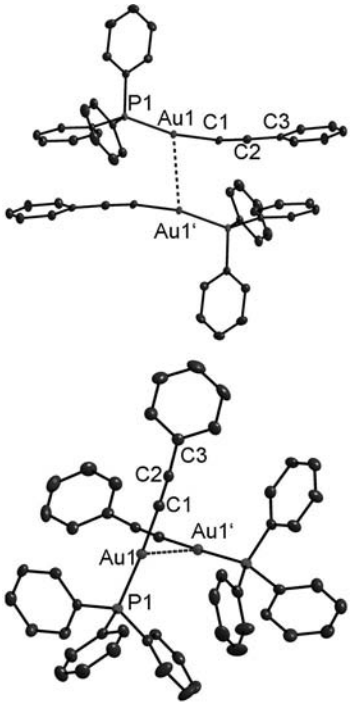

Figure 1. Molecular structures of the neutral Au^{I} complexes [Au(R^2)PPh_3] (top) and [Au(R^1)PPh_3] (bottom). Hydrogen atoms omitted for clarity. Vibrational ellipsoids drawn at the 50% probability level. Selected bond lengths [pm] and angles [°] for [Au(R^2)-PPh_3]: Au1–P1 228.04(9), Au1–C1 199.5(3), C1–C2 121.0(4), C2–C3 143.5(4), Au1···Au1′ 327.74(14); P1–Au1–C1 167.55(10), Au1–C1–C2 170.3(3), C1–C2–C3 177.7(3). Selected bond lengths [pm] and angles [°] for [Au(R^1)PPh_3]: Au1–P1 228.52(11), Au1–C1 200.7(4), C1–C2 120.6(5), C2–C3 143.9(5), Au1···Au1′ 295.06(6); P1–Au1–C1 174.42(11), Au1–C1–C2 176.4(4), C1–C2–C3 175.5(4).

(1)[Au(C≡CAr)$_2$]$_2$ (Type II)

The crystal structures of (**1**)[Au(R^1)$_2$]$_2$ and (**1**)[Au(R^2)$_2$]$_2$ are similar. We shall first discuss the structure of (**1**)[Au-(R^2)$_2$]$_2$ in some detail, based on the illustrations in Figures 2 and 3. From Figure 2 one can see that the Au atoms are arranged in the form of condensed, curled six-membered rings, remotely resembling the packing of P atoms in black phosphorus. The Au···Au separations in these hexagons are large (682.9–726.5 pm) and, thus, there clearly is no direct bonding between the Au atoms. The dashed lines drawn in the figures do not symbolise bonding interactions, but instead highlight the packing motif. The Au atoms of two adjacent layers are *in-phase* (directly on top of each other). The acetylido ligands are oriented perpendicularly to the layer plane. Four slightly different anionic Au complex units were found within the unit cell, featuring Au–C bond lengths in the range 197.9(6)–200.2(6) pm. The C–Au–C bond angles cover the range 172.2(2)–177.3(2)°. The $\mathbf{1}^{2+}$ units are located in the centre of each hypothetical Au_6 hexagon. The unit cell contains three slightly different units of $\mathbf{1}^{2+}$. The variations in the C–C bond lengths within the central C_6 rings [137.9–149.5, 138.6(6)–151.1(7) and 139.1–150.9(7) pm for the three different units of **1**] clearly indicate loss of aromaticity (see the Lewis structure for $\mathbf{1}^{2+}$ in Scheme 3). As already mentioned, the crystal structure of (**1**)[Au(R^1)$_2$]$_2$ (see Figure 4) is similar to that of (**1**)[Au-(R^2)$_2$]$_2$. However, the hexagons with Au atoms in the corners are considerably elongated in (**1**)[Au(R^1)]$_2$, and the Au···Au separation varies from 686.8(3) and 846.0(6) pm.

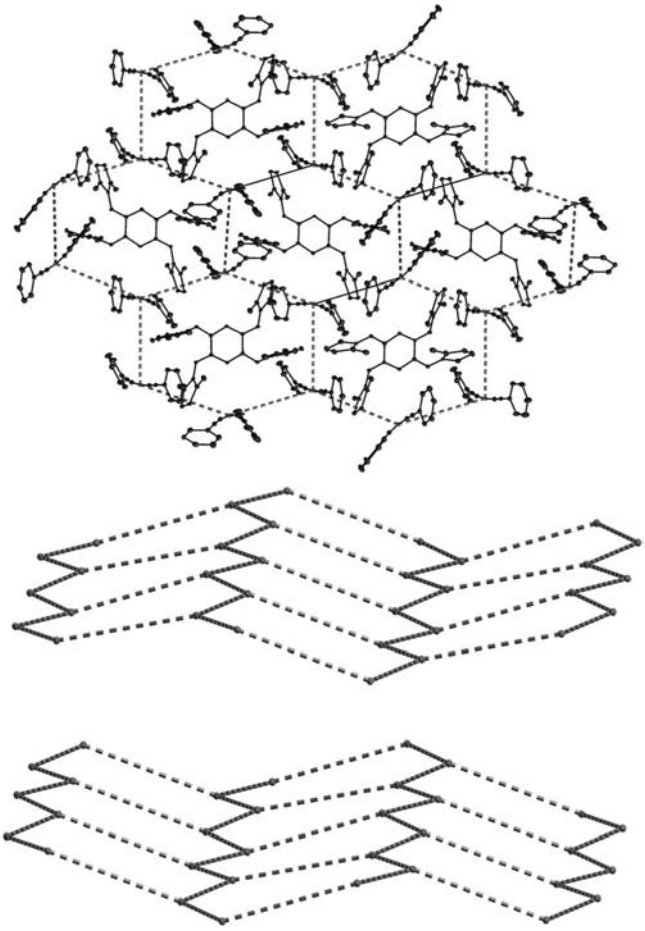

Figure 2. (top) Section of the crystal structure of (**1**)[Au(R^2)$_2$]$_2$ showing one of the layers; hydrogen atoms omitted for clarity; the dashed lines connecting the Au atoms have no chemical meaning but should assist the description of the structure. (bottom) Arrangement of the Au atoms in two adjacent layers; all other atoms are omitted.

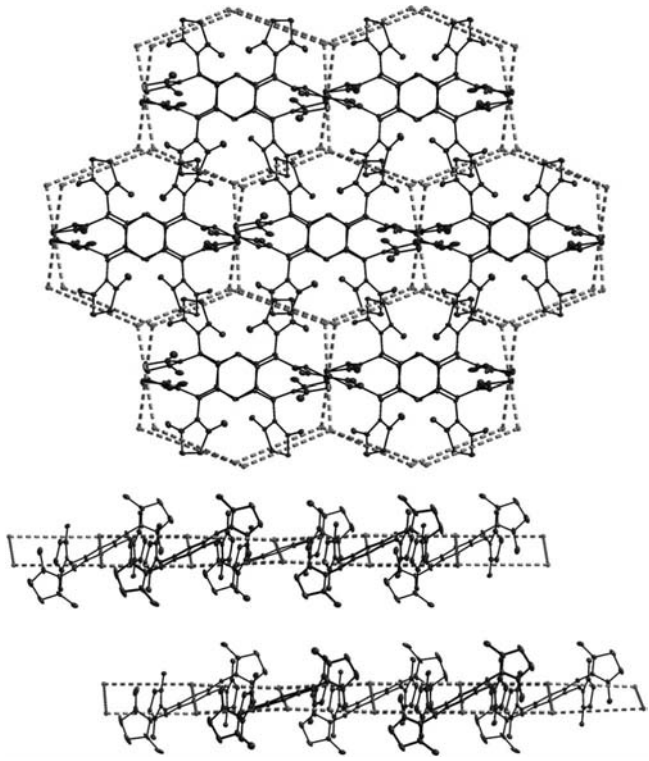

Figure 3. View (in two directions) of two adjacent layers in crystalline (**1**)[Au(R^2)$_2$]$_2$. The acetylido ligands and all hydrogen atoms are omitted for clarity.

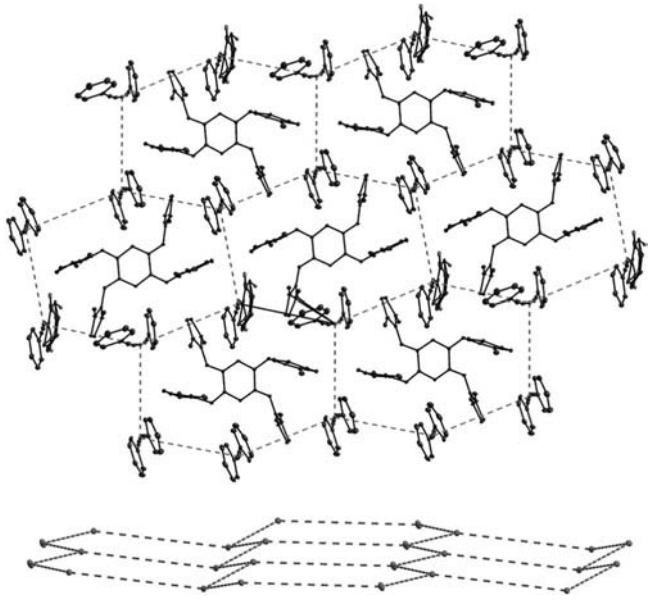

Figure 4. (top) Section of the crystal structure of (**1**)[Au(R^1)$_2$]$_2$ showing one of the layers; hydrogen atoms omitted for clarity; the dashed lines connecting the Au atoms have no chemical meaning but should assist the description of the structure. (bottom) Arrangement of the Au atoms in one layer; all other atoms are omitted.

The salt (**1**)[Au(R^3)$_2$]$_2$ adopts a completely different structure, which is illustrated in Figure 5. The crystal is clearly built of units each consisting of the dication (**1**)$^{2+}$ and two [Au(R^3)$_2$]$^-$ anions. These units are then packed in a way such that rows of the dications and rows of the anions result (each row of **1**$^{2+}$ is followed by two rows of [Au(R^3)$_2$]$^-$). Finally, we isolated a small quantity of crystals of the salt (**1**)$_3$[Au(R^4H)$_2$]$_2$Cl$_4$ (see Figure 6) from the reaction between [AuCl(PPh$_3$)], R^4H_2 and **1**. The chlorido ligands establish hydrogen bonds to the acetylido units. Unfortunately, it was not possible (despite several attempts) to improve the yield of this interesting product.

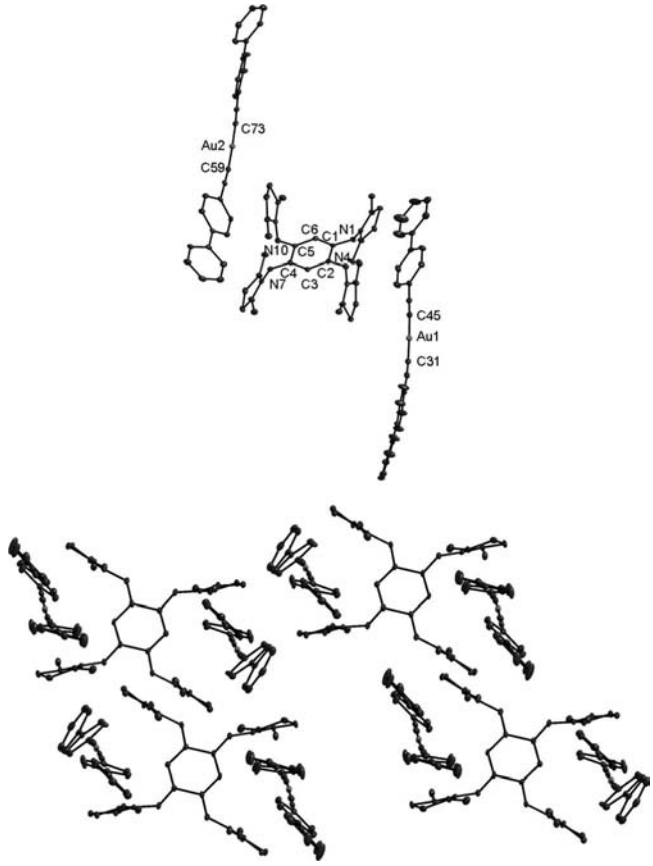

Figure 5. Section of the crystal structure of (**1**)[Au(R^3)$_2$]$_2$. Hydrogen atoms omitted for clarity. (top) One of the layers; the dashed lines connecting the Au atoms have no chemical meaning but should assist the description of the structure. (bottom) Arrangement of the Au atoms; all other atoms are omitted.

Thermal Conversions and Properties of (1)[Au(R^1)$_2$]$_2$

The crystals of (**1**)[Au(R^1)$_2$]$_2$ are of a dark blue-black, shiny appearance (see the photo provided in the Supporting Information), while the powder material is yellow-green. In Figure 7, the absorption spectrum of a CH_3CN solution of (**1**)[Au(R^1)$_2$]$_2$ is compared with the solid-state spectrum. The spectrum of the solution displays relatively intense bands at 240, 292 (with signs of vibrational progression) and 419 nm. The region between 450 and 750 nm in the solution spectrum is enlarged to show the presence of another broad band around 614 nm. The spectrum of the solid material contains absorptions with maxima at $\lambda \approx 460$ and 630 nm. We also assessed the electrical conductivity of

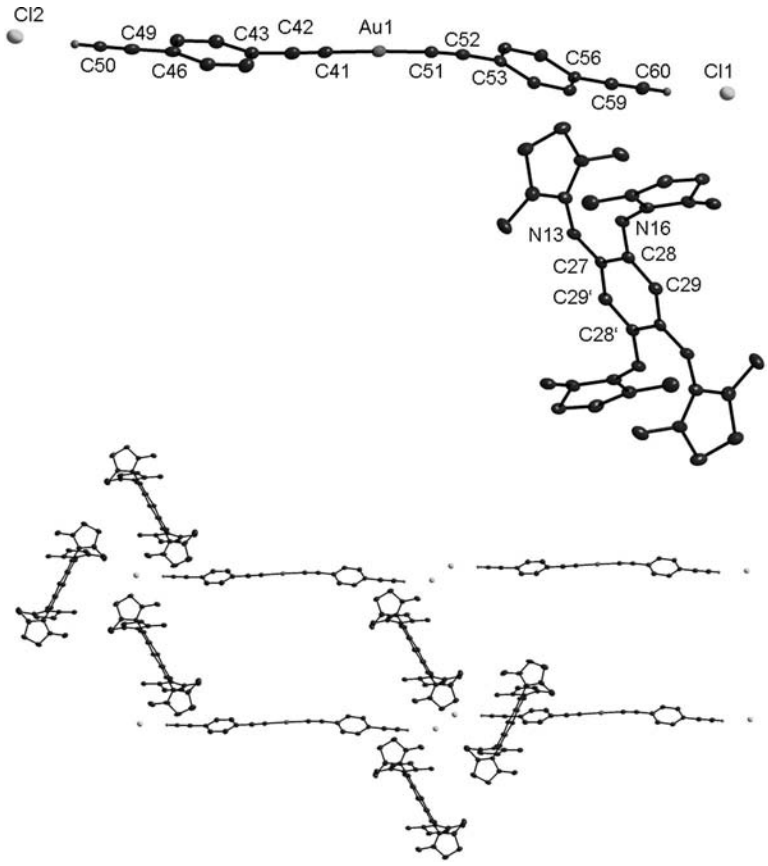

Figure 6. Molecular structure of $(\mathbf{1})_3[Au(R^4H)_2]_2Cl_4$. All hydrogen atoms except for the acetylene ones are omitted for clarity. The chlorido ligands are engaged in hydrogen bonding with the acetylene hydrogen atoms as well as water molecules (not visualised).

$(\mathbf{1})[Au(R^1)_2]_2$ in the temperature range 30–180 °C (the melting point is reached above 200 °C), but it turned out to be too small to be measurable. In further experiments, the thermal stability of $(\mathbf{1})[Au(R^1)_2]_2$ was studied with thermogravimetric (TG) and differential scanning calorimetric (DSC) measurements. In Figure 8 the DSC and TG curves recorded for $(\mathbf{1})[Au(R^1)]_2$ are displayed. The large and relatively sharp exothermic peak in the DSC curve at 227 °C, which immediately follows the endothermic melting peak, arises from a reaction associated with a reaction energy of approximately –280 kJ mol^{-1}. To obtain more information about the product of this conversion, the solid material was dissolved after heat treatment to 250 °C in CD_2Cl_2 (yielding a red solution with a black residue) and analysed by using NMR spectroscopy (see spectra in the Supporting Information). The spectra show the reformation of neutral **1** upon heating of $(\mathbf{1})[Au(R^1)_2]_2$ [signals at δ = 2.63 (s, 24 H, CH_3), 3.15 (s, 16 H, CH_2) and 6.06 (s, 2 H, H_{Ar}) ppm in the ^{1}H NMR spectrum of a CD_2Cl_2 solution]. The TG curve indicates a small mass loss associated with this process. To obtain additional information, the volatile decomposition products released from $(\mathbf{1})[Au(R^1)_2]_2$ upon heating were collected on a cold finger (kept at ca. 10 °C). A white solid was obtained, which can be completely dissolved in CD_2Cl_2. According to NMR spectroscopy, it consists of a mixture of neutral **1** and the 1,3-diacetylene $(PhC{\equiv}C)_2$.[10] The $(PhC{\equiv}C)_2$ was also clearly visible in the high-resolution mass spectra recorded for the white solid [*m*/*z* (%) = 202.079 (100), 203.080 (20.3), 204.084 (1.8)]. The thermally induced coupling of the acetylido ligands of each $(\mathbf{1})[Au(C{\equiv}CAr)_2]_2$ releases four electrons, which are spent for reduction of the two Au^I ions and the dication $\mathbf{1}^{2+}$. The thermal decomposition can thus be described by the equation given in Scheme 6.

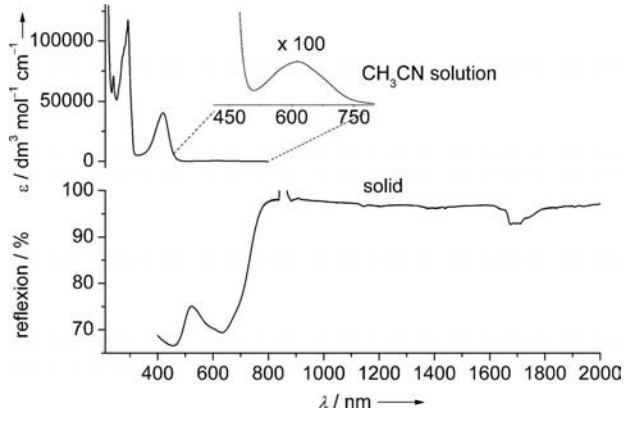

Figure 7. Comparison between the UV/Vis/NIR spectra recorded for $(\mathbf{1})[Au(R^1)_2]$ in a CH_3CN solution and in the solid state. The region between λ = 450 and 750 nm in the solution spectrum is enlarged to show the weak and broad band centred at 614 nm.

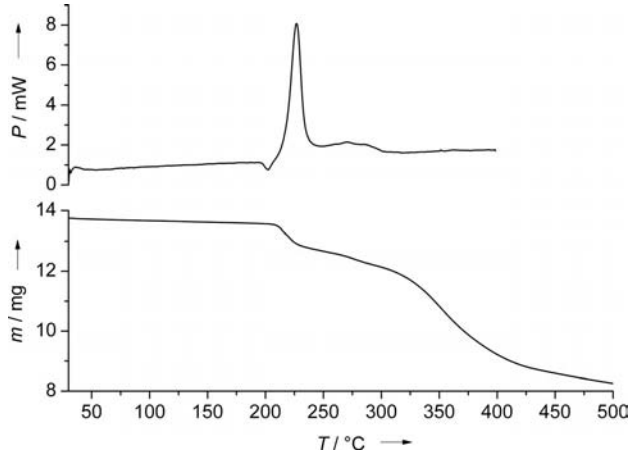

Figure 8. DSC (top) and TG (bottom) curves (N_2, heating rate 5 K min^{-1}) measured for solid (**1**)[Au(R^1)$_2$].

Scheme 6.

Conclusions

The reaction between [AuCl(PPh$_3$)] and several acetylenes ArC≡CH (Ar = phenyl, pyridinyl, biphenyl or *p*-acetylphenyl) in the presence of the guanidine base and organic electron donor **1** yielded two different product types, namely the neutral gold complexes [Au(C≡CAr)PPh$_3$] and the salts (**1**)[Au(C≡CAr)$_2$]$_2$. The presence of both product types shows a competition between the deprotonation {[Au(C≡CAr)PPh$_3$]} and the redox channels {(**1**)[Au(C≡CAr)$_2$]$_2$} of the reaction. As anticipated from the large differences in the polarity between both product types, they can be easily separated from each other by crystallisation under different conditions. The yields largely depend on the acetylene used.

Furthermore, the optical properties and thermal decomposition of the salt (**1**)[Au(C≡CPh)$_2$]$_2$ were analysed in detail. The absorption spectrum of the solid material features several low-lying electronic excitations. Measurements on the electrical conductivity indicate a large resistivity. The salt decomposes at 227 °C in an exothermic reaction (ca. –280 kJ mol^{-1}). This decomposition results in oxidative coupling of the two acetylido ligands. The electrons released in this coupling are consumed on reformation of the neutral guanidine **1** and formation of the gold clusters.

In Scheme 7 the reactions of [AuCl(PPh$_3$)] with acetylenes and acetonitrile in the presence of the strong base and electron donor **1** are summarised. Interestingly, the redox channel may not be observed at all in the reaction with acetonitrile but was found to be of considerable importance in the reaction with the stronger C−H-acidic acetylenes. In future work we will study further reactions of [AuCl(PPh$_3$)] with weak proton acids mediated by **1** or other guanidine-functionalised compounds, which are at the same time strong Brønsted bases and redox-active.

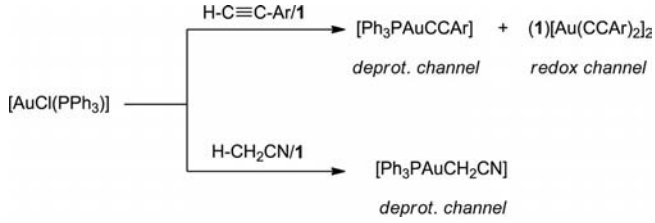

Scheme 7.

Experimental Section

General: The reactions were carried out under argon by applying standard Schlenk techniques. All solvents were rigorously dried prior to use. The preparation of **1** was carried out as described in the literature.[6] IR and UV/Vis/NIR measurements were carried out with a BioRad Merlin Excalibur FTS 3000 and a Varian Cary 5000 machine, respectively. NMR spectra were recorded with a Bruker Avance II 400 or an Avance DPX AC200 spectrometer. Elemental analyses were carried out at the Microanalytical Laboratory of the University of Heidelberg. EI mass spectra were measured with a Finnigan MAT 8230 or with a JEOL JMS-700 instrument.

[Au(R^1)(PPh$_3$)] and (1)[Au(R^1)$_2$]$_2$: 1 (100 mg, 0.19 mmol) was dissolved in CH_3CN (10 mL). Then [AuCl(PPh$_3$)] (189 mg, 0.38 mmol) and R^1H (0.2 mL, 1.82 mmol) were added. The solution was stirred at 90 °C for 22 h. Subsequently, the reaction mixture was allowed to cool to room temp. and filtered. The filtrate was kept at 4 °C for 12 h, during which time dark blue-black crystals of (**1**)[Au(R^1)$_2$]$_2$ precipitated. Yield: 81 mg (0.08 mmol, 41%). The solution was filtered and the filtrate stored at 4 °C. After a few days, pale-yellow crystals of [Au(R^1)(PPh$_3$)] appeared. Yield: 102 mg (0.18 mmol, 47%).

[Au(R^1)(PPh$_3$)]

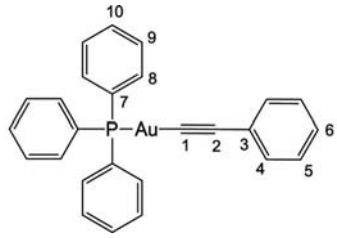

$C_{26}H_{20}AuP$ (560.38): calcd. C 55.73, H 3.60, P 5.53; found C 55.92, H 3.58, P 5.56. ^{1}H NMR (600 MHz, CD_2Cl_2): δ = 7.27 (m, 3 H, H_{Ar}), 7.56 (m, 17 H, H_{Ar}) ppm. ^{13}C NMR (150 MHz, CD_2Cl_2): δ = 103.63 (s), 121.74 (s), 125.93 (s), 127.12 (s), 128.59 (s), 129.67 (d, $J_{C,P}$ = 11.27 Hz, C9), 130.38 (d, $J_{C,P}$ = 55.77 Hz, C7), 132.13 (d, $J_{C,P}$ = 2.33 Hz, C10), 132.50 (s), 134.74 (d, $J_{C,P}$ = 13.83 Hz, C8) ppm. ^{31}P NMR (242 MHz, CD_2Cl_2): δ = 42.17 ppm. IR (CsI): $\tilde{\nu}$ = 3061 (m), 2118 [m, ν(C≡C)], 1596 (w), 1483 (m), 1435 (m), 1310 (w), 1214 (w), 1018 (w), 1161 (w), 1101 (m), 1065 (w), 1025 (m), 996 (m), 912 (w), 755 (s), 691 (s), 618 (w), 534 (s), 510 (s), 438 (m) cm^{-1}. MS (FAB): *m*/*z* (%) = 560.9 (60) [M]$^+$, 458 (84) [Au(PPh$_3$)]$^+$, 139 (100). Crystal data: $C_{52}H_{40}Au_2P_2$, M_r = 1120.72, 0.45 × 0.45 × 0.40 mm, monoclinic, space group *C*2/*c*, *a* = 22.040(4), *b* = 17.205(3), *c* = 14.703(3) Å, β = 125.99(3)°, *V* = 4511(2) Å^3, *Z* = 4, $d_{calcd.}$ = 1.650 Mg m^{-3}, Mo-K_α radiation (graphite-monochromated, λ = 0.71073 Å), *T* = 100 K, θ_{range} = 1.64–33.10°. Reflections measured 16232, independent reflections 8543, R_{int} = 0.0488. Final *R* indices [$I > 2\sigma(I)$]: R_1 = 0.0359, wR_2 = 0.0679.

(1)[Au(R^1)$_2$]$_2$

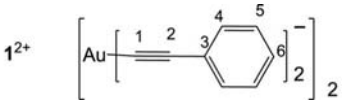

$C_{58}H_{62}Au_2N_{12}$ (1321.13): calcd. C 52.73, H 4.73, N 12.72; found C 52.67, H 4.62, N 12.78. ^{1}H NMR (600 MHz, CD_2Cl_2): δ = 2.84 (s, 24 H, CH_3), 3.75 (s, 8 H, CH_2), 4.15 (s, 8 H, CH_2), 5.59 (2 H, H_{Ar}), 7.17 (m, 20 H, H_{Ar}) ppm. ^{13}C NMR (150 MHz, CD_2Cl_2): δ = 33.26 (s, *C*H$_3$), 48.65 (s, *C*H$_2$), 74.40 (s, Au*C*C), 95.56 (s, AuC*C*), 120.34 (s), 122.00 (s), 123.72 (s), 123.72 (s), 125.92 (s), 128.48 (s), 132.06 (s) ppm. IR (CsI): $\tilde{\nu}$ = 2872 (w), 2375 (w), 2101 [m, ν(C≡C)], 1566 (w), 1507 (m), 1462 (m), 1410 (m), 1347 (vs), 1284 (s), 1024 (s), 972 (m), 909 (w), 843 (w), 757 (s), 694 (m) cm^{-1}. UV/Vis (CH_3CN, 3.78×10^{-5} mol L^{-1}): λ (ε) = 292 (117350), 240 (70888), 419 (40377 L mol^{-1} cm^{-1}) nm. MS (FAB): *m*/*z* (%) = 522.2 (100) [**1**]$^+$, 622.3 [**1** + R^1 + H]$^+$, 921.3 [**1** + AuR^1]$^+$, 1220.0 [**1** + 2 Au + 3 R^1 + H]$^+$. Crystal data: $C_{58}H_{62}Au_2N_{12}$, M_r = 1321.14, $0.40\times0.36\times0.36$ mm, monoclinic, space group *P*2(1), *a* = 15.110(3), *b* = 19.702(4), *c* = 17.894(4) Å, β = 94.43(3)°, *V* = 5311.1(19) Å^3, *Z* = 4, $d_{calcd.}$ = 1.652 Mg m^{-3}, Mo-K_α radiation (graphite-monochromated, λ = 0.71073 Å), *T* = 100 K, θ_{range} = 1.14–30.05°. Reflections measured 30681, independent reflections 30644, R_{int} = 0.0384. Final *R* indices [$I > 2\sigma(I)$]: R_1 = 0.0406, wR_2 = 0.0769.

[Au(R^2)(PPh$_3$)] and (1)[Au(R^2)$_2$]$_2$: Guanidine **1** (52 mg, 0.10 mmol) was dissolved in CH_3CN (10 mL), and [AuCl(PPh$_3$)] (100 mg, 0.20 mmol) and R^{2}H (41 mg, 0.40 mmol) were added. The reaction mixture was stirred at 90 °C for 22 h. Subsequently, it was allowed to cool to room temp. and filtered. The filtrate was kept at room temp. for 1–2 d, during which time pale-yellow crystals of [Au(R^2)(PPh$_3$)] precipitated. Yield: 41.5 mg (0.07 mmol, 37%). The solution was filtered and the filtrate stored at 4 °C. After a few days, dark blue-black crystals of (**1**)[Au(R^2)$_2$]$_2$ formed. Yield: 42 mg (0.03 mmol, 33%).

[Au(R^2)(PPh$_3$)]

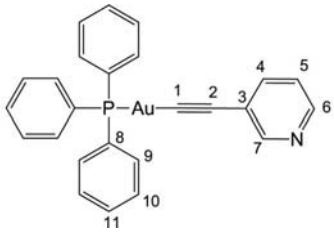

$C_{25}H_{19}AuNP$ (561.09): calcd. C 53.49, H 3.41, N 2.50, P 5.52; found C 53.53, H 3.39, N 2.55, P 5.55. ^{1}H NMR (600 MHz, CD_2Cl_2): δ = 7.17 (dd, 1 H, pyridine H5), 7.53 (m, 15 H, PPh_3-H), 7.68 (dt, 1 H, pyridine H4), 8.38 (dd, 1 H, pyridine H6), 8.61 (d, 1 H, pyridine H7) ppm. ^{13}C NMR (150 MHz, CD_2Cl_2): δ = 100.22 (s), 122.86 (s), 123.30 (s) 129.74 (d, $J_{C,P}$ = 11.35 Hz, C10), 130.27 (d, $J_{C,P}$ = 56.14 Hz, C8), 132.20 (d, $J_{C,P}$ = 2.43 Hz, C11), 134.83 (d, $J_{C,P}$ = 13.83 Hz, C9), 139.13 (s), 147.47 (s), 153.38 (s) ppm. ^{31}P NMR (242 MHz, CD_2Cl_2): δ = 41.96 ppm. IR (CsI): $\tilde{\nu}$ = 2960 (w), 2114 (m), 1579 (w), 1559 (w), 1479 (s), 1435 (s), 1403 (s), 1317 (w), 1262 (m), 1226 (m), 1185 (m), 1161 (w), 1101 (s), 1025 (m), 996 (m), 916 (w), 848 (w), 803 (s), 751 (vs), 700 (vs), 625 (w), 578 (m), 534 (vs), 510 (vs), 438 (m) cm^{-1}. MS (FAB): *m*/*z* (%) = 300.0 (20) [Au(R^2) + H]$^+$, 459.0 (90) [Au(PPh$_3$)]$^+$, 562.0 (100) [Au(R^2)PPh$_3$ + H]$^+$. UV/Vis (CH_3CN, $c = 1.02\times10^{-4}$ mol L^{-1}): λ (ε) = 236 (35290), 269 (26103), 280 (21976 L mol^{-1} cm^{-1}) nm. Crystal data: $C_{25}H_{19}AuNP$, M_r = 561.35, $0.45\times0.40\times0.40$ mm, triclinic, space group $P\bar{1}$, *a* = 8.8570(18), *b* = 9.5340(19), *c* = 13.444(3) Å, *α* = 69.54(3)°, β = 72.39(3)°, γ = 78.67(3)°, *V* = 1008.6(4) Å^3, *Z* = 2, $d_{calcd.}$ = 1.848 Mg m^{-3}, Mo-K_α radiation (graphite-monochromated, λ = 0.71073 Å), *T* = 100 K, θ_{range} = 3.16–30.06°. Reflections measured 10689, independent reflections 5858, R_{int} = 0.0195. Final *R* indices [$I > 2\sigma(I)$]: R_1 = 0.0252, wR_2 = 0.0664.

(1)[Au(R^2)$_2$]$_2$

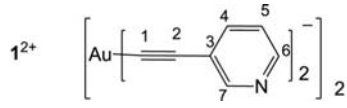

$C_{54}H_{58}Au_2N_{16}$ (1324.4): calcd. C 48.95, H 4.41, N 16.91; found C 48.83, H 4.45, N 16.71. ^{1}H NMR (600 MHz, CD_2Cl_2): δ = 2.84 (s, 24 H, CH_3), 3.76 (s, 8 H, CH_2), 4.08 (s, 8 H, CH_2), 5.54 (s, 2 H, H_{Ar}), 7.11 (dd, 4 H, pyridine H5), 7.58 (dt, 4 H, pyridine H4), 8.29 (dd, 4 H, pyridine H6), 8.45 (d, 4 H, pyridine H7) ppm. ^{13}C NMR (150 MHz, CD_2Cl_2): δ = 33.34 (s, *C*H$_3$), 48.66 (s,*C*H$_2$), 99.02 (s,C_{Ar}−H), 107.16 (s), 123.30 (s), 124.56 (s), 124.92 (s), 138.68 (s), 146.40 (s), 153.03 (s), 158.73 (s), 164.65 (s) ppm. IR (CsI): $\tilde{\nu}$ = 2935 (w), 2106 [m, ν(C≡C)], 1624 (s), 1571 (s), 1507 (vs), 1467 (s), 1407 (m), 1350 (s), 1278 (m), 1222 (m), 1181 (w), 1157 (w), 1093 (w), 1025 (s), 972 (m), 803 (m), 735 (w), 707 (w), 582 (w), 506 (m) cm^{-1}. UV/Vis (CH_3CN, $c = 2.08\times10^{-5}$ mol L^{-1}): λ (ε) = 219 (96416), 239 (62769), 297 (83822), 420 (36671 L mol^{-1} cm^{-1}) nm. MS (FAB): *m*/*z* (%) = 403.3 (12) [Au(R^2)$_2$ + 2 H]$^+$, 522.6 (100) [**1**]$^+$, 924.0 (26) [**1** + Au(R^2)$_2$ + H]$^+$, 1222.1 (6) [**1** + Au(R^2)$_2$ + Au(R^2) + 2 H]$^+$. MS (ESI$^-$, MeOH): *m*/*z* (%) = 401.9 (100) [Au(R^2)$_2$]$^-$. MS (ESI$^+$, MeOH): *m*/*z* (%) = 260.8 (100) [**1** – 2 H]$^{2+}$, 922.3 (86) [**1** + Au(R^2)$_2$ – H]$^+$. Crystal data: $C_{54}H_{58}Au_2N_{16}$, M_r = 1325.10, $0.35\times0.33\times0.30$ mm, triclinic, space group $P\bar{1}$, *a* = 14.049(3), *b* = 14.288(3), *c* = 26.919(5) Å, *α* = 88.05(3)°, β = 89.27(3)°, γ = 76.25(3)°, *V* = 5246(2) Å^3, *Z* = 4, $d_{calcd.}$ = 1.678 Mg m^{-3}, Mo-K_α radiation (graphite-monochromated, λ = 0.71073 Å), *T* = 100 K, θ_{range} = 0.76–30.06°. Reflections measured 53025, independent reflections 30460, R_{int} = 0.0529. Final *R* indices [$I > 2\sigma(I)$]: R_1 = 0.0494, wR_2 = 0.0993.

[Au(R^3)(PPh$_3$)] and (1)[Au(R^3)$_2$]$_2$: AuClPPh$_3$ (100 mg, 0.20 mmol) and R^{3}H (74.5 mg, 0.40 mmol) were added to a solution of **1** (52 mg, 0.10 mmol) in CH_3CN (10 mL). The solution was stirred at 90 °C for 22 h. Subsequently, the solution was cooled to room temp. and filtered. The filtrate was kept at room temp. for 1–2 d, during which time pale-yellow crystals of [Au(R^3)(PPh$_3$)] formed. Yield 16 mg (0.026 mmol, 13%). The solution was filtered and the filtrate stored at 4 °C for several days. Dark-blue crystals of (**1**)[Au(R^3)$_2$]$_2$ formed. Yield: 3 mg (2%).

[Au(R^3)(PPh$_3$)]

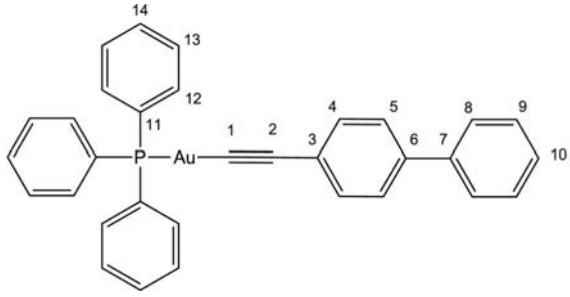

$C_{32}H_{24}AuP$ (636.45): calcd. C 60.39, H 3.80; found C 60.10, H 3.82. ^{1}H NMR (600 MHz, $CDCl_3$): δ = 7.27 (t, 1 H, H_{Ar}10), 7.49 (m,

23 H, H_{Ar}) ppm. ^{13}C NMR (150 MHz, CD_2Cl_2): δ = 103.37 (s), 121.15 (s), 124.99 (s), 127.22 (s), 127.36 (s), 127.84 (s), 129.33 (s), 129.74 (d, $J_{C,P}$ = 11.28 Hz, C13), 130.42 (d, $J_{C,P}$ = 55.84 Hz, C11), 132.16 (d, $J_{C,P}$ = 2.13 Hz, C14), 132.97 (s), 134.86 (d, $J_{C,P}$ = 13.84 Hz, C12), 139.71 (s), 141.11 (s) ppm. ^{31}P NMR (242 MHz, CD_2Cl_2): δ = 42.32 ppm. IR (CsI): $\tilde{\nu}$ = 3062 (w), 2110 (w), 1600 (w), 1485 (m), 1435 (m), 1218 (w), 1101 (m), 1025 (w), 844 (m), 751 (m), 691 (s), 578 (m), 538 (vs), 498 (s) cm^{-1}. MS (FAB): *m/z* (%) = 77.1 (24) $[Ph]^+$, 262.3 (100) $[PPh_3]^+$, 459.4 (5) $[AuPPh_3]^+$. Crystal data: $C_{32}H_{24}AuP$, M_r = 636.45, 0.15 × 0.10 × 0.10 mm, triclinic, space group $P\bar{1}$, a = 10.021(2), b = 12.404(3), c = 12.560(3) Å, α = 100.58(3)°, β = 111.13(3)°, γ = 113.21(3)°, V = 1238.0(4) $Å^3$, Z = 2, $d_{calcd.}$ = 1.707 $Mg\,m^{-3}$, Mo-K_α radiation (graphite-monochromated, λ = 0.71073 Å), T = 100 K, θ_{range} = 1.88–30.02°. Reflections measured 13323, independent reflections 7158, R_{int} = 0.0362. Final R indices [$I > 2\sigma(I)$]: R_1 = 0.0336, wR_2 = 0.0633.

(1)[Au(R³)₂]₂

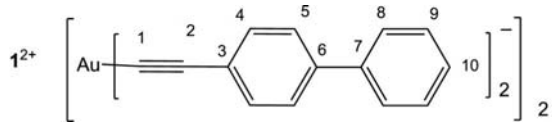

$C_{82}H_{78}Au_2N_{12}{\cdot}H_3CCN$ (1666.55): calcd. C 60.54, H 4.90, Au 23.64, N 10.93; found C 60.30, H 4.75, N 10.13. ^1H NMR (600 MHz, CD_2Cl_2): δ = 2.87 (s, 24 H, CH_3), 3.59 (s, 8 H, CH_2), 4.43 (s, 8 H, CH_2), 5.58 (s, 2 H, H_{Ar}), 7.38 (m, 4 H, H_{Ar}10), 7.46 (m, 8 H, H_{Ar}9), 7.64 (m, 24 H, H_{Ar}4,5,8) ppm. Yield too low for ^{13}C NMR spectroscopy. IR (CsI): $\tilde{\nu}$ = 3027 (w), 2959 (w), 2873 (w), 2102 (m), 1616 (s), 1570 (s), 1509 (vs), 1408 (m), 1350 (s), 1282 (s), 1099 (m), 1026 (m), 973 (m), 803 (m), 705 (m), 694 (m), 557 (w), 502 (w) cm^{-1}. UV/Vis (CH_3CN, $c = 5.29 \times 10^{-5}$ $mol\,L^{-1}$): λ (ε) = 20 (15649), 321 (19581), 419 (5093 $L\,mol^{-1}\,cm^{-1}$) nm. MS (ESI^-, MeOH): *m/z* (%) = 551.3 (100) [Au – $(R^3)_2$]$^-$. MS (ESI^+, MeOH): *m/z* (%) = 261.4 (27) [**1** + H]$^{2+}$, 522.3 (100) [**1**]$^+$. Crystal data for: $C_{84}H_{81}Au_2N_{13}$, M_r = 1666.55, 0.20 × 0.15 × 0.15 mm, triclinic, space group $P\bar{1}$, a = 14.165(3), b = 16.138(3), c = 16.774(3) Å, α = 103.15(3)°, β = 93.31(3)°, γ = 108.50(3)°, V = 3505.6(12) $Å^3$, Z = 2, $d_{calcd.}$ = 1.579 $Mg\,m^{-3}$, Mo-K_α radiation (graphite-monochromated, λ = 0.71073 Å), T = 100 K, θ_{range} = 2.01–27.40°. Reflections measured 29171, independent reflections 15749, R_{int} = 0.0666. Final R indices [$I > 2\sigma(I)$]: R_1 = 0.0516, wR_2 = 0.0866.

(1)[Au(R⁴)₂]₂

[AuCl(PPh_3)] (100 mg, 0.20 mmol) and R^4H_2 (50.5 mg, 0.40 mmol) were added to a solution of **1** (52 mg, 0.10 mmol) in CH_3CN (10 mL). The reaction mixture was then stirred at 90 °C for 22 h. Subsequently, the solution was cooled down to room temp. and filtered. Storage of the green filtrate at 4 °C led to a colourless precipitate of polymeric $[Au_2R^4]_n$, which newly formed even after several cycles of filtration. The polymer was identified from the mass spectrum of the precipitate (ESI^- (MeOH): *m/z* (%) = 447.2 (100) [Au$(R^4)_2$]$^-$, 904.9 (31) [$Au_2(R^4)_4$]$^-$.) Upon layering of a CH_3CN solution with (not rigorously dried) Et_2O, a small quantity of green crystals of (**1**)$_3$[Au$(R^4H)_2]_2Cl_4$ (containing Et_2O as well as H_2O molecules) was obtained, in addition to further polymeric $[Au_2R^4]_n$. Crystal data: $C_{123.6}H_{160}Au_2Cl_4N_{36}O_{8.7}$, M_r = 2825.02, 0.20 × 0.15 × 0.15 mm, monoclinic, space group $P2_1/c$, a = 29.545(6), b = 13.291(3), c = 17.943(4) Å, β = 94.93(3)°, V = 7020(3) $Å^3$, Z = 2, $d_{calcd.}$ = 1.337 $Mg\,m^{-3}$, Mo-K_α radiation (graphite-monochromated, λ = 0.71073 Å), T = 100 K, θ_{range} = 2.28–27.50°. Reflections measured 31351, independent reflections 16010, R_{int} = 0.0731. Final R indices [$I > 2\sigma(I)$]: R_1 = 0.0664, wR_2 = 0.1518.

X-ray Crystallographic Study: Suitable crystals were taken directly out of the mother liquor, immersed in perfluorinated polyether oil, and fixed on top of a glass capillary. Measurements were carried out with a Nonius-Kappa CCD diffractometer with a low-temperature unit by using graphite-monochromated Mo-K_α radiation. The temperature was set to 200 K. The data collected were processed by using the standard Nonius software.[11] All calculations were performed by using the SHELXT-PLUS software package. Structures were solved by direct methods with the SHELXS-97 program and refined with the SHELXL-97 program.[12,13] Graphical handling of the structural data during solution and refinement was performed with XPMA.[14] Structural representations were generated by using Winray 32.[15] Atom coordinates and anisotropic thermal parameters of non-hydrogen atoms were refined by full-matrix least-squares calculations. CCDC-812254 [Au$(R^1)PPh_3$], -812255 (**1**)[Au$(R^4)_2]_2$, -812256 (**1**)[Au$(R^2)_2]_2$, -812257 [Au$(R^2)PPh_3$], -812258 (**1**)[Au$(R^1)_2]_2$, -812259 [Au$(R^3)PPh_3$], and -812260 (**1**)[Au$(R^3)_2]_2$ contain the supplementary crystallographic data for this paper. These data can be obtained free of charge from The Cambridge Crystallographic Data Centre via www.ccdc.cam.ac.uk/data_request/cif.

Supporting Information (see footnote on the first page of this article): Photo of crystals of (**1**)[Au$(R^1)_2]_2$, molecular structure of [Au$(R^3)PPh_3$], NMR spectra recorded before and after thermal decomposition of (**1**)[Au$(R^1)_2]_2$.

Acknowledgments

The authors wish to thank N. Wagner and Prof. Dr. Johannes Beck, University Bonn, for conductivity measurements and fruitful discussions. Financial support from the Deutsche Forschungsgemeinschaft (DFG) is gratefully acknowledged.

[1] a) H. Schmidbaur, *Chem. Soc. Rev.* **1995**, *24*, 391–400; b) D. M. P. Mingos, *J. Chem. Soc., Dalton Trans.* **1996**, 561–566; P. Pyykkö, *Angew. Chem.* **2004**, *116*, 4512–4557; *Angew. Chem. Int. Ed.* **2004**, *43*, 4412–4456.
[2] J. Vicente, J. Gil-Rubio, N. Barquero, P. G. Jones, D. Bautista, *Organometallics* **2008**, *27*, 646–659.
[3] J. Vicente, M. T. Chicote, *Coord. Chem. Rev.* **1999**, *193–195*, 1143–1161.
[4] a) J. Vicente, M.-T. Chicote, I. Saura-Llamas, M. C. Lagunas, *J. Chem. Soc., Chem. Commun.* **1992**, 915–916; b) J. Vicente, M.-T. Chicote, M.-D. Abrisqueta, *J. Chem. Soc., Dalton Trans.* **1995**, 497–498; c) J. Vicente, M. T. Chicote, M. D. Abrisqueta, M. C. Ramírez de Arellano, *Organometallics* **2000**, *19*, 2968–2974; d) J. Vicente, M.-T. Chicote, M. M. Alvarez-Falcón, *Organometallics* **2003**, *22*, 4792–4797; e) J. Vicente, M.-T. Chicote, M. M. Alvarez-Falcón, *Organometallics* **2005**, *24*, 2764–2772.
[5] D. Emeljanenko, A. Peters, V. Vitske, E. Kaifer, H.-J. Himmel, *Eur. J. Inorg. Chem.* **2010**, 4783–4789.
[6] A. Peters, E. Kaifer, H.-J. Himmel, *Eur. J. Org. Chem.* **2008**, 5907–5914.
[7] C. Paal, C. Amberger, *Ber. Dtsch. Chem. Ges.* **1905**, *38*, 1394–1397.
[8] M. I. Bruce, D. N. Duffy, *Aust. J. Chem.* **1986**, *39*, 1697–1701.
[9] L. Gao, D. V. Partyka, J. B. Updegraff III, N. Deligonul, T. G. Gray, *Eur. J. Inorg. Chem.* **2009**, 2711–2719.
[10] See, for example: A. Coste, F. Couty, G. Evano, *Synthesis* **2010**, 1500–1504.
[11] HKL2000 (Demo-SMN), Data Processing Software, Nonius, **1998**, http://www.nonius.nl.

[12] a) G. M. Sheldrick, *SHELXS-97, Program for Crystal Structure Solution*, University of Göttingen, **1997**, http://shelx.uni-ac.gwdg.de/SHELX/index.html; b) G. M. Sheldrick, *SHELXL-97, Program for Crystal Structure Refinement*, University of Göttingen, **1997**, http://shelx.uni-ac.gwdg.de/SHELX/index.html.
[13] *International Tables for X-ray Crystallography*, Kynoch Press, Birmingham, U. K., **1974**, vol. 4.
[14] L. Zsolnai, G. Huttner, *XPMA*, University of Heidelberg, **1994**, http://www.uni-heidelberg.de/institute/fak12/AC/huttner/software/software.html.
[15] R. Soltek, *Winray 32*, University of Heidelberg, **2000**, http://www.uni-heidelberg.de/institute/fak12/AC/huttner/software/software.html.

Received: February 18, 2011
Published Online: June 1, 2011

